This is the peer-reviewed version of the article:

B. J. Malešević, M. Petrović, M. Obradović, and B. Popkonstantinović, ‘On the extension of the Erdös-Mordell type inequalities’, *Mathematical Inequalities & Applications*, vol. 17, no. 1, pp. 269–281, 2014, doi: 10.7153/mia-17-22.

# Vehicle swept path analysis based on GPS data

Vladan Ilić [a, *], Dejan Gavran [a, 1], Sanja Fric [a, 2], Filip Trpčevski [a, 3], and Stefan Vranjevac [a, 4]

[a] *Department for Roads, Railroads, and Airports, Faculty of Civil Engineering University of Belgrade, Belgrade 11000, Serbia,*

[*] Corresponding author, Tel: +381640266582, Fax: +381113370223, E-mail addresses: vilic@grf.bg.ac.rs, and vla.ilic@yahoo.com,

[1] E-mail address: gavran@eunet.rs

[2] E-mail address: sfric@grf.bg.ac.rs

[3] E-mail address: ftrpcevski@grf.bg.ac.rs

[4] E-mail address: svranjevac@grf.bg.ac.rs

**Abstract:** Vehicle swept path analysis presents an essential step while working on at-grade intersection and roundabout designs. Following the intensive development of computer-aided design (CAD) software in the past two decades, numerous CAD-based computer programs for vehicle movement simulation have been developed and commercially distributed. The accuracy of these simulation programs is usually verified by conducting experimental field tests in which real movement trajectories of design vehicles, equipped with global positioning system (GPS) receivers, are recorded. This paper proposes an improved methodology for retrieving vehicle movement trajectories from collected GPS data. The proposed methodology reduces the trajectory inaccuracy resulting from pavement grading characteristics and the inability to accurately install GPS receivers in relation to streamlined vehicle body. Results of field experiments show that the reduction of positioning errors in the horizontal projection is not smaller than 50.0 mm compared with previous studies.

**Keywords**: off-tracking, vehicle movement trajectory, GPS receiver, grading plan, 3D triangle

# Introduction

Rear wheels of a vehicle negotiating a tight curve within a crossroad never follow trajectories of corresponding front wheels. The effect of the rear wheels trajectories' inward displacement is known as off-tracking and has major influence on the positioning of curbs and traffic isles. Vehicles with a longer wheelbase (the distance between the leading/datum point and rear axle) produce larger off-tracking while negotiating a curve (Harwood et al. 2003). Leisch and Carrasco (2014) made a comprehensive chronological overview of vehicle swept path analysis, from its inception in the late 1930s, and provided insight into its future developments.

According to the most relevant road design standards in Europe (FGSV 2006; VSS 2003), the design vehicle is designated as a vehicle that requires the largest road space to perform a turning maneuver without encroaching adjacent traffic lanes or climbing onto curbs. Hence, dimensional and kinematic characteristics of the critical vehicle have a profound effect on an intersection's layout. In the USA, the AASHTO Green Book (2011) has established 19 design vehicles in four different classes (passenger cars, buses, trucks, and recreational vehicles). Drivers of long vehicles, such as articulated lorries and other combination vehicles with more articulation points, frequently have to perform complex maneuvers in order to comply with geometrical limitations imposed by intersection layout plans. This problem is most evident at compact roundabouts (Pecchini et al. 2017; Rubio-Martin et al. 2015) and four-leg at-grade intersections with acute intersecting angles (Korlaet et al. 2010). Dragčević et al. (2005) showed that curbs set along the right edges at at-grade intersections are commonly damaged by vehicles performing right turns.

In the last 70 years, many mathematical models describing critical vehicles' movement trajectories have been developed (WHI 1970; Woodrooffe et al. 1983; Sayers 1991; Wang and Linnett 1995). Using modern Global Navigation Satellite System (GNSS) technologies all these mathematical procedures could be checked in real conditions.

## Review of experimental methods for retrieving vehicle movement trajectories

Full-scale field tests still represent the most accurate and reliable method for retrieving vehicle movement trajectories. The key advantage of practical driving tests is that all potential parameters, such as drivers' skills, vehicle speed, and road conditions, are implicitly taken into account. Nevertheless, the preparation and conducting of these tests are usually time-consuming and require considerable financial resources. In Europe, standardized and internationally accepted procedures for conducting field tests do not exist yet (Pecchini and Giuliani 2013), whereas in the USA, the Society of Automotive Engineers (SAE) (2011) established a field test procedure to determine maximum off-tracking and minimum turning diameters of motor vehicles.

The most practical and efficient method for conducting filed tests is using design vehicles equipped with water tanks installed on the vehicle body. Besides water, colored liquids and paints could be poured into the tanks and used to mark swept paths directly on the dry pavement surface. Video recordings, combined with image processing, and utilization of global positioning system (GPS) instrumentation are used to analytically retrieve multiple swept paths painted on the pavement. Mussone et al. (2011) proposed a method for the analysis of vehicle movements in roundabouts based on image processing.

Field experiments using large vehicles on roadways with different turning angles and geometric features were conducted by Cheng and Huang (2011). Turning paths of wheels and operations of the steering wheel were recorded. The results of field experiments were compared with those of a computational method.

Recently, many researchers tried to determine vehicle movement trajectories with the help of GPS receivers mounted on top of test vehicles. In an influential study, Pecchini and Giuliani (2013), analyzed the movement of an articulated lorry through a roundabout. In their experiment, GPS devices were installed on the vehicle to provide trajectories of the most prominent points of the lorry, and using these data, real swept path envelopes were recorded.

The same maneuvers were then simulated using the AutoTURN software (2017) and the results were compared with field test envelopes, in order to verify the software's reliability. The precision level provided by the deployed GPS positioning techniques in this experimental study was limited to 100.0 mm.

Extensive research of heavy vehicles' trajectories at at-grade intersections and roundabouts, using GPS technology was done by Friedrich et al. (2013). In this study, the points on curbs, encroached by the most prominent parts of heavy vehicles' bodies, were identified.

The software company "Transoft solutions" conducted field tests to check vehicle movement trajectories by using GPS receivers installed on the top of specially configured vehicles. Trajectories of the front and rear axles of wind blade trailers were recorded (Frost 2014). Flores at al. (2015) also compared the swept paths of wind blade trailers from the field experiment with software-simulated maneuvers. They found a main source of discrepancy between swept path envelopes, obtained using AutoTURN, and field tests in possible misspecification of the exact locations of the GPS receivers on the truck and trailer. Accurate recording of vehicle swept path envelopes under real conditions represents a hot topic for all companies developing computer programs for road and intersection design. These companies need reliable and efficient methods to test the accuracy of software tools for vehicle swept path analyses.

However, the vast majority of tests deploying GPS technology have not taken into account the specific morphology (grading characteristics) of the pavement surface. Additionally, in previous field experiments the positions of GPS receivers installed on test vehicles have been assessed by simple measurements of relative distances in relation to the vehicle cabin or wheel hubs, which is another source of considerable errors.

# Identification of the problem and proposed methodology

Retrieving the path of even slow moving vehicles from GPS data looks attractive at first glance. But, not taking into account even the slightest undulations of the pavement surface (in the order of 1% to 2%) causes considerable errors. Moreover, accurate mounting of GPS receivers on the vehicle cabin or superstructure might be difficult; conversely, retrieving the vehicle path from inaccurately positioned GPS receivers results in inaccurate trajectories. Encountering these problems in the field, an improved methodology was developed, which is based on the following input (known) data:

- Steering path, trajectory of a vehicle datum point;
- Dimensions and kinematic parameters of a vehicle;
- Triangulated model (TIN) of the pavement at the test polygon.

Initially, accurate positions of GPS receivers on the vehicle body are unknown. GPS receivers are installed on the vehicle approximately, and their accurate positions will be retrieved in the office, using new software. Thus, based on the above-mentioned input data, the following steps are executed in office:

- Projecting positions of GPS receivers traveling a few meters above the pavement (e.g., on top of a cabin) normally onto the pavement surface (TIN model), i.e. retrieving real GPS trajectories in plan projection.
- Assuming that the datum point (front bumper center, in this case) accurately follows the steering path in plan projection, and geometrically correlating GPS receivers' horizontal projections to that steering path, accurate GPS positions on the vehicle's body are retrieved. Only at this point GPS positions on the vehicle become known.
- Based on the known positions of GPS receivers on the vehicle, vehicle symbols (graphical blocks) are superimposed over sets (pairs) of GPS positions in a CAD environment, thus retrieving the instances of a vehicle at consecutive intervals (usually at 100.0 mm intervals).

## Preparation of the field experiment

### Test polygon

The field experiment was carried out on a large truck parking area within a private complex of an international transport company located in the municipality of Surčin, 20 km from the Serbian capital Belgrade. The available parking space for test drives was 100 m long and 80 m wide, with the asphalt pavement in very good condition, without any bumps or surface defects. The pavement surface was dry and cleared of debris.

The steering path alignment consisted of two curves with radii of 12.5 m and 15.0 m, respectively. The tangent arrangement provided for turn angles between 60° and 180°. The configuration of the test polygon is given in Fig. 1a. All key points, e.g., curves' entries, tangent points, and radii, were accurately marked on the pavement surface using a total station and an electronic theodolite. To precisely delineate the alignment, additional points were interpolated along both circular and tangent elements, at 1.0 m intervals. Finally, points on the pavement surface were connected by a special wear-resistant red duct tape.

The grading plan of the test field was generated from the triangulated irregular network-TIN 3D model. Fig. 1b shows the grading plan with a 0.05 m contour interval, as well as the water flow lines.

**Fig. 1.**

**Test vehicles**

Four types of large vehicles were selected for the field test. The first one was a lorry with an overall length of 16.50 m, composed of a Volvo FH 500 tractor and a 13.70 m long Schmitz semitrailer, with three fixed axles. The second vehicle was a classic heavy Renault T430 truck in a three axle configuration, which pulled a KRONE central axle tandem trailer. For this type of truck, the second axle was powered by the engine (the third axle was lifted during test drives), while the first axle was the only one with a steering function. These two types of heavy vehicles were selected as most frequent on the Serbian rural highway network.

On the other hand, the articulated bus and single city bus are typical for Serbian urban transport. The articulated bus Solaris URBINO 18 which was used in the experiment was 18.00 m long and its first axle was the only steerable one. As a representative of single-unit vehicles, a classic two-axle city bus Ikarbus IK 112 was selected. Fig. 2 illustrates key dimensions of the test vehicles.

**Fig. 2.**

In addition, the positioning of GPS receivers mounted on vehicles' bodies is also displayed in Fig. 2. For the Volvo FH 500, two GPS receivers were installed on top of the tractor cabin and two on top of the semitrailer's rigid side wall structure. For the Renault T430, two GPS receivers were installed on the frame of the truck's curtainsider superstructure; another two were installed on the supporting aluminum profiles on top of the trailer.

Two GPS receivers were mounted on the top of the front and one on the rear segment of Solaris articulated bus. For the single unit city bus, only two GPS receivers were needed on the top of the vehicle.

**GNSS measurement system**

High precision real time GNSS service provided by the Active Geodetic Reference Network of Serbia (AGROS) was used in the experiment for the collection of GPS data. Configurable Trimble R8s receivers, with two integrated Maxwell 6 chips and 440 GNSS channels for advanced high-accuracy satellite tracking, were installed on vehicles' bodies and connected to notebook computers equipped with Trimble Access Field and Trimble Business Center software for acquisition, checking, and processing of GPS data. To obtain almost continuous vehicle trajectory recordings, a recording frequency of 10 Hz was used, as recommended by Glabsch et al. (2012) and Sun et al. (2017). The precision level of the measurement system with the postprocessing of acquired data is between 8.0 and 15.0 mm in the horizontal plane.

The application of the described GNSS system required full-time coverage of no less than four satellites during testing. In total, four GPS receivers, accompanied with four notebook computers, were used for all test runs. The Trimble R8s GPS receiver, installed on the top of bus body, is shown in Fig. 2.

**Test runs execution and vehicle guidance techniques**

The experiment was conceived so that a particular vehicle follows the steering trajectory marked on the pavement surface by its most prominent central point: usually, front bumper center. This was conducted by installing a high-power laser designator on the front bumper center and an action camera just above, pointed at the laser beam and transmitting video recordings in real time, via a Wi-Fi connection, to the tablet mounted in front of the driver (attached to the inner side of the windshield) (Fig. 3). Vehicles were driven by experienced drivers who carefully guided the green laser beam (Fig. 4d) emitted by the laser designator (Fig.

4c), over the steering trajectories, and by looking at live-stream recordings from the camera (Fig. 4b) transmitted to the tablet in the cabin (Fig. 4a).

**Fig. 3.**

For every turning maneuver and for each vehicle, test runs were executed twice. Vehicle speed was strictly controlled by an electronic cruise control system (tempomat) and limited to 10.0 km/h, so the drivers did not have to struggle to maintain constant speed and could concentrate on guiding the vehicle.

**Fig. 4.**

# Experiment results and discussion

**Retrieving single-unit vehicle trajectories from GPS coordinates**

The first problem after installing the GPS receivers was how to determine the exact position of GPS antennas relative to the vehicle body. As shown in Fig. 5, due to the streamlined surface of the Volvo FH 500 cabin, it is practically impossible to determine the distances between the installed GPS receivers and the key points of the cabin (especially in plan view). Exact positioning of GPS receivers could be possible only in high-tech vehicle testing centers. Therefore, even the positions of GPS receivers within the vehicle's coordinate system had to be calculated later in the office, by comparing GPS receivers' trajectories to the steering path.

**Fig. 5.**

After processing the GPS data, horizontal coordinates in the Serbian national (Gauss-Krueger) coordinate system were obtained. For every vehicle unit, except the second segment of the articulated bus (which requires one coordinate pair, or one receiver only), data sets composed of two X, Y coordinate pairs (one pair for each GPS receiver), at 0.1 s intervals (10 Hz positioning rate), were generated and saved in .txt files. Afterwards, a simple routine named GPS2LINE, written in the AutoLISP programming language, was deployed; it takes pairs of points (pairs of X, Y coordinates), each corresponding to a particular truck position (every 0.1 s), imports them in AutoCAD and connects them with lines (entities named GPSLINES). Fig. 6 shows what

GPSLINES, obtained from the data set generated for the Volvo FH 500 tractor, looks like when drawn in the AutoCAD environment.

**Fig. 6.**

The grading plan (Fig 1b), shows that the surface of the pavement at the test polygon is not ideally flat (horizontal). In order to satisfy minimal drainage requirements, the surface was constructed with small longitudinal and cross grades. Furthermore, to ensure a stable connection with GPS navigation satellites serving the GNSS system, GPS receivers had to be installed on the top of the vehicle body. While the steering alignment was marked right on the pavement surface, installed GPS receivers were traveling high above the pavement, e.g., in the case of the Volvo FH 500 tractor, two Trimble R8s receivers were traveling 3.82 m above the pavement surface. This elevation difference between the position of the GPS receivers and the guiding trajectories certainly had an effect on the measurement accuracy. GPS receiver positions had to be projected normally onto the pavement surface. This was done by creating a new AutoLISP routine called LIN2TRI, which takes previously generated GPSLINES, projects their endpoints normally onto the pavement 3D triangles and moves them up the triangles' gradients (Fig 7).

**Fig. 7.**

If the two 3D triangles below the two GPS receivers belong to two different planes $\Pi_1$ and $\Pi_2$, which are defined by the following general equations:

$$\Pi_1 = a_1x + b_1y + c_1z + d_1 \tag{1}$$

$$\Pi_2 = a_2x + b_2y + c_2z + d_2 \tag{2}$$

the endpoints of GPSLINES are projected onto the planes ($\Pi_1$ and $\Pi_2$) with different gradient vectors $\overrightarrow{v_1}$ and $\overrightarrow{v_2}$. The first task for the LIN2TRI routine to execute is to determine the 3D triangle to which the planar projection of the GPS receiver ($G_{1h}$ or $G_{2h}$) belongs. Then, points $G_{1h}$ and $G_{2h}$ are moved up along the gradient vectors $\overrightarrow{v_1}$ and $\overrightarrow{v_2}$, respectively, to their new positions marked $G_1$ and $G_2$. Actually, points $G_1$ and $G_2$ represent normal (not vertical) projections of GPS receivers onto planes $\Pi_1$ and $\Pi_2$. If the angle between the normal vector of plane $\Pi_1$ and the vertical line starting from the point $GPS_1$ is defined as $\theta_1$, the $X_1$ and $Y_1$ coordinates of the shifted point $G_1$ are calculated as

$$X_1 = X_{1h} - a_1 \cdot H_{GPS} \cdot \tan(\theta_1) \quad (3)$$

$$Y_1 = Y_{1h} - b_1 \cdot H_{GPS} \cdot \tan(\theta_1) \quad (4)$$

where $H_{GPS}$ represents the elevation difference between point $GPS_1$ in the center of the GPS receiver and the pavement surface. The angle $\theta_1$ can be obtained from plane parameters (equation (1)), using a simple analytical formula:

$$\theta_1 = \arccos\left(\frac{c_1}{\sqrt{a_1^2 + b_1^2 + c_1^2}}\right) \quad (5)$$

Coordinates $X_2$ and $Y_2$ for the point $G_2$ are calculated the same way. After applying the LIN2TRI routine, all imported GPSLINES were shifted in relation to the gradient vectors of the corresponding 3D triangles representing the pavement surface.

Now, GPS receiver positions refer to the pavement surface, and not to the top of the vehicle. But, even the precise positions of the GPS receivers within the vehicles' coordinate system are still unknown. However, one thing was for sure: for every GPSLINE (for every position of the vehicle) the frontal centerpoint of the vehicle (datum point) was laying exactly on the steering path marked on the pavement surface. Therefore, a new command MIDLIN was introduced which draws lines (MIDLINES) starting from GPSLINES' midpoints, with a length d and angle $\gamma$ in relation to the corresponding GPSLINE (Fig. 8). MIDLINES connect the points laying midway between GPS receivers with the corresponding datum points. The next command developed was the LINMOD command which colectively modifies all selected MIDLINES, giving them a new length d and a new angle $\gamma$ relative to the corresponding GPSLINE. By applying the LINMOD command in sequence, the user adjusts the d and $\gamma$ parameters, so the frontal endpoint of every MIDLINE overlaps with the steering path. Thus, by trial and error, the frontal endpoint of every MIDLINE, which acts as a laser beam is put in the right place.

**Fig. 8.**

By now, it is known at what distance d and angle $\gamma$, the frontal center of the vehicle rests, relative to the midpoint of a line connecting the two GPS receivers. However, the lower left portion of Fig. 9 shows that there is an infinite number of GPS receivers' positions satisfying these two exact parameters. One can imagine the truck rotating around the frontal center point;

then, there is one specific angle α between the MIDLINE and the longitudinal axis of the truck which finally defines the GPS receivers' positions whitin the corrdinate system of the truck. In order to finally resolve this problem, the series of truck positions imediatelly before the curved section of the steering path is taken into acount. Here, at the end of the entrance tangent, the truck was stopped and its alignment checked prior to the maneuver. The longitudinal truck axis was always overlapping the entrance tangent in concern fairly well. At this location, a series of GPSLINES was processed using the AVGLINE command which takes GPSLINES and generates an "average" line having the average azimuth and laying in the center of gravity of all selected GPSLINES. Having the angle between the AVGLINE (the line connecting two GPS receivers) and the longitudinal truck axis (entrance tangent) on one side, and the angle γ between the AVGLINE (as a representative of GPSLINES) and the MIDLINE on another, the angle α between the MIDLINE and the longitudinal truck axis is retreived. The final step is creating an AutoCAD block representing the truck with the insertion point in the midpoint of the GPSLINE and (slightly) rotated for the angle α in relation to the MIDLINE's frontal endpoint. The block is supposed to meet the following requirements:

- frontal center point must overlap with the outer (frontal) MIDLINE endpoint (datum point);
- the block (longitudinal truck axis) is rotated for the angle α around the frontal center point, in relation to the MIDLINE;
- the midpoint of the GPSLINE is formally taken as the block insertion point (the importance of this formality is elaborated in the next paragraph).

Finally, the command VEH2LINE takes truck blocks and overlaps them over all GPSLINES representing that particular vehicle.

**Fig. 9.**

There was an alternative solution for retreiving the angle α between the MIDLINE and the longitudinal truck axis. The command ALPHA takes two consecutive instances of MIDLINES and calculates the angle α from them. The program behind ALPHA is based on the fact that the point at the distance equal to the wheelbase (BASE on Fig. 10) from the datum point is always directed towards the leading point L. While the leading point L (front center, datum point) moves from $L_i$ to $L_{i+1}$, covering a step k, the trailing point (the point located at the distance equal to the wheelbase behind the leading point) is directed to the midpoint of step k. Using simple geometric relations, acute angles $\varphi_1$, $\varphi_2$, $\beta_1$, and $\beta_2$ are calculated as

$$\varphi_1 = 180° - \eta - \alpha \tag{6}$$

$$\varphi_2 = \eta - \xi - \delta \tag{7}$$

$$\beta_1 = 180° - (\xi + \alpha + \delta) \tag{8}$$

$$\beta_2 = \xi + \alpha + \delta \tag{9}$$

**Fig. 10.**

Applying the law of sines on the two characteristic triangles from two consecutive vehicle positions, the set of two equations follows:

$$\frac{k/2}{\sin\varphi_2} = \frac{\mathrm{BASE}}{\sin\beta_2} \tag{10}$$

$$\frac{k/2}{\sin\delta} = \frac{\mathrm{BASE}}{\sin\beta_1}$$

Bearing in mind that $\beta_1 = 180° - \beta_2$ and $\sin\beta_1 = \sin(180° - \beta_2) = \sin\beta_2$, the only realistic solution for the system of equations (10) is

$$\beta_2 = \arcsin\left(\frac{\mathrm{BASE}}{k/2} \cdot \sin\delta\right) \tag{11}$$

$$\sin\varphi_2 = \sin\delta \tag{12}$$

Then, the angle $\alpha$ is derived from equations (9) and (11) as:

$$\alpha = \arcsin\left(\frac{\mathrm{BASE}}{k/2} \cdot \sin\delta\right) - \xi - \delta \tag{13}$$

The methodology described above, presented for the Volvo FH 500 tractor is identical for any other single-unit vehicle. Therefore, swept path envelopes for the Renault T430 heavy truck, for the first segment of the Solaris URBINO 18 articulated bus, and for the Ikarbus IK 112 city bus are retrieved in the same way.

**Retrieving trailer trajectories from GPS coordinates**

Identical methods and AutoLISP routines used for the single unit vehicle (Volvo FH tractor) swept path analysis could be reapplied for the trailer swept path analyses. Unlike the leading vehicle (tractor), which follows the steering path by its frontal center point, the semitrailer follows the dragging path of the tractor's fifth wheel by its kingpin. Fig. 11a shows a SCHMITZ semitrailer following the Volvo FH 500 tractor and how the semitrailer's MIDLINES are forced to follow the tractor's fifth wheel, by adjusting the $\gamma_s$ and $d_s$ parameters.

Finally, the same command AVGLINE was used to determine the angle $\alpha_s$ between the semitrailer's MIDLINE and its longitudinal axis (Fig. 11b). The AVGLINE routine is applied on GPSLINES located just in front of the curved portion of the steering path (the end of the entrance tangent), where the semitrailer's longitudinal axis is aligned with the tangent. Thus, knowing the angle between the GPSLINE and the entrance tangent (semitrailer's longitudinal axis) on one hand, and the angle $\gamma_s$ between the GPSLINE and MIDLINE on the other, the angle $\alpha_s$ between the MIDLINE and semitrailer's longitudinal axis is retrieved.

**Fig. 11.**

Now, the semitrailer's block is created with the kingpin identical to the MIDLINE's frontal end point and rotated for $\alpha_s$ relative to MIDLINE. Just as in the tractor's case, the insertion point of the block is formally placed in the GPSLINE's midpoint. Semitrailer's blocks are automatically overlapped over the semitrailer's GPSLINES using the VEH2LINE routine (Fig. 12b), just like the tractor's blocks were overlapped over their own GPS positions (Fig. 12a).

**Fig. 12.**

In the semitrailer's case it is of the outmost importance to put the insertion point in GPSLINE's midpoint, though the philosophy of contemporary vehicle movement simulations within AutoCAD is based on blocks inserted at a datum point (MIDLINE's frontal point in this case). It is very important to notice that all of the tractor's GPSLINES are almost identical in length. Unlike the tractors body (cabin), the semitrailer's superstructure is much more elastic. While traveling over the uneven pavement surface, the semitrailer's top twists, stretches, and compresses. In contrast to the tractor's GPSLINES whose lengths are 1.61 m (for the Volvo FH

500), the SCHMITZ semitrailer's GPSLINES ($L_{GPS_S}$ in Fig. 11a) vary between 13.47 m and 13.51 m. To cope with this source of error, it is best to put the semitrailer's insertion point in the middle of the GPSLINE and not in one of its endpoints or the MIDLINE's frontal point.

**Fig. 13.**

The same methodology applied for the SCHMITZ semitrailer hooked directly to the tractor, could be, in sequence, reapplied for any additional trailer hooked on the trailer already pulled by the leading vehicle (Fig. 13). Hence, the methodology presented herein could be used for unlimited compositions of vehicles.

**Implementation of the methodology and accuracy improvements**

By not taking into account realistic morphology of the pavement surface, GPS position error can grow from 30.0-40.0 mm, for a general pavement grade of 1%, to 60.0-80.0 mm for pavements with grades in the order of 2%. Table 1 shows the error in X, Y terms with no pavement grading characteristics taken into account.

**Table 1.**

It can be seen that as the GPS receiver is set at a higher altitude and as the grade of the pavement at test field is higher, the positioning error in the horizontal projection will be greater. Furthermore, the methodology presented herein overcomes the inability to accurately install GPS receivers on curved cabins of modern trucks; it allows the GPS receivers to be installed only approximately, while their accurate positions are recalculated in the office, by kinematically relating their absolute X, Y coordinates to the steering path. As a consequence, accuracy is further enhanced and workload in the field is reduced at the expense of the development/deployment of simple AutoLISP software tools.

# Conclusion

In recent years, retreiving vehicle swept paths using kinematic GNSS systems has become a common tool for checking the accuracy and reliability of modern CAD-based vehicle movement simulations. Most published methodologies are characterized by two major drawbacks: the inability to accurately position the GPS receiver atop the streamlined vehicle body and ignoring the true grading characteristics of the test polygon. The methodology presented herein is essentially based on the unknown positions of GPS receivers within the vehicle's coordinate system. Precise GPS receiver's positions on the vehicle are retreived by kinematically comparing GPS receiver's trajectories with the elements of the steering path. As a result, it became possible to automatically overlap vehicle blocks over the GPS receivers' positions. Also, using elementary spatial geometry relations, GPS receivers' positions were projected from the top of the vehicle down to the pavement surface, further improving accuracy.

Major improvements compared with previous GPS field measurements of real vehicle movement trajectories are:

- accurate assessment of GPS receivers' positions on the streamlined cabins of modern trucks;
- reduced costs for experiment preparation, because there is no need for devising specially fabricated tools for accurate positioning of GPS receivers in relation to the cabin sides, windshield, axels, or some other parts of the vehicle body;
- by taking into account the grading characteristics of the pavement surface at test polygon, the positioning errors in the horizontal projection (X, Y coordinates) are reduced by more than 50.0 mm for each tested vehicle.

As a final result, the workload in the field and the time necessary for preparing future experiments are reduced, as the accurate positions of GPS receivers on a vehicle's body are retrieved later in the office, by correlating GPS positions to the steering path. Also, this methodology can be very helpful to producers and developers of CAD-based simulation software tools for the experimental testing of the accuracy and reliability of their products.

# References

AASHTO (American Association of State Highway and Transportation Officials). 2011. A Policy on Geometric Design of Highways and Streets. 6th ed., Washington, D.C.

Autoturn Pro 3D [Computer Software]. 2017. Richmond, BC, Canada, Transoft Solutions.

Cheng, J.F., and Huang, H.C. 2011. Effects of Roadway Geometric Features on Low-Speed Turning Maneuvers of Large vehicles. International Journal of Pavement Research and Technology, **4**(6): 373 - 383.

Dragčević, V., Korlaet, Ž., Rukavina, T., and Lakušić, S. 2005. Three - leg Intersection at - Grade - The Right Edge Forming Test. *In* Proceedings of the 3rd International Symposium on Highway Geometric Design, Compendium of papers, Chicago, Illinois, 29 June - 1 July 2005. Transportation Research Board (TRB), Washington D.C., CD-ROM, 16 p.

FGSV (German Road and Transportation Research Association) 2006. German standard FGSV-Nr. 200: RASt - Richtlinien für die Anlage von Stadtstraßen. Cologne, Germany.

Flores, J., Chan, S., and Homola, D. 2015. A Field Test and Computer Simulation Study on the Wind Blade Trailer. *In* Proceedings of the 5th International Symposium on Highway Geometric Design, Compendium of papers, Vancouver, Canada, 22-24 June 2015. Transportation Research Board (TRB), Washington D.C., CD-ROM, 17p.

Friedrich, B., et al. 2013. Überprüfung der Befahrbarkeit innerörtlicher Knotenpunkte mit Fahrzeugen des Schwerlastverkehrs. Forschungsprojekt FE 77.0501/2010, Schlussbericht - im Auftrag des Bundesministers für Verkehr, Bau und Stadtentwicklung, Institut für Verkehr und Stadtbauwesen und Institut für Geodäsie und Photogrammetrie, Technische Universität Braunschweig und SHP Ingenieure GbR Hannover, Deutschland. (in German). Available from http://www.bast.de/DE/Verkehrstechnik/Fachthemen/v1-lang-lkw/Berichte/770501.html [accessed 14 March 2017].

Frost, M. 2014. Improving the Modeling of OSOW Movements through Filed Test Studies. Rapid City - 2014th Joint Western/Midwestern ITE District Annual Meeting, Session 1D - Oversized Trucks in Roundabouts, 29 June - 1 July 2014. Institute of Transportation Engineers (ITE), SD, USA. Available from https://www.westernite.org/annualmeetings/14_Rapid_City/Presentations/1D-Frost.pdf [accessed 23 January 2018].

Glabsch, J., Heunecke, O., Schuhbäck, S., and Wirth. W. 2012. Swept path determination by means of PDGNSS. *In* Proceedings of the 3rd International Conference on Machine Control & Guidance - MCG, 27 - 29 March 2012, Stuttgart, Germany. Available from http://www.uni-stuttgart.de/ingeo/mcg2012/proceedings.htm [accessed 17 February 2017].

Harwood, D.W, et al. 2003. Review of Truck Characteristics as Factors in Roadway Design. National Cooperative Highway Research Program, NCHRP Report 505, Transportation Research Board. Washington D.C. Available from http://www.trb.org/Publications/Blurbs/153579.aspx [accessed 25 February 2017].

Korlaet, Ž., Dragčević, V., and Stančerić, I. 2010. Designing Criteria of Acute Angle Four-Leg Intersection at Grade. *In* Proceedings of the 4th International Symposium on Highway Geometric Design, Valencia, Spain, 2 - 5 June 2010. Polytechnic University of Valencia and Transportation Research Board, Washington, D.C., 15p.

Leisch, J.P., and Carrasco, M. 2014. Design Vehicles: From Turning Templates to Smart Systems. *In* Proceedings of 2014 Conference & Exibition, Transportation 2014: Past, Present, Future, Montreal, Canada, 28 September - 1 October. Transportation Association of Canada (TAC), 20p. Available from http://conf.tac-atc.ca/english/annualconference/tac2014/english/papers_by_author.htm [accessed 2 March 2017].

Mussone, L., Matteucci, M., Bassani, M., and Rizzi, D. 2013. An innovative method for the analysis of vehicle movements in roundabouts based on image processing. Journal of Advanced Transportation, **47**(6): 581-594. DOI:10.1002/atr.184

Pecchini, D., and Giuliani, F. 2013. Experimental Test of an Articulated Lorry Swept Path. ASCE Journal of Transportation Engineering, **139**(12): 1174 - 1183. Available from http://dx.doi.org/10.1061/(ASCE)TE.1943-5436.0000601 [accessed 13 January 2017].

Pecchini, D., Roncella, R., Forlani, G., and Giuliani, F. 2017. Measuring driving workload of heavy vehicles at roundabouts. Transportation Research Part F: Traffic Psychology and Behaviour, **45**(2017): 27-42. doi:10.1016/j.trf.2016.11.010

Rubio-Martin, J.L., Jurado-Piña, R., and Pardillo-Mayora, J.M. 2015. Heuristic procedure for the optimization of speed consistency in the geometric design of single-lane roundabouts. Canadian Journal of Civil Engineering, **42**(1): 13-21. doi:10.1139/cjce-2014-0283.

SAE (Society of Automotive Engineers) 2011. Turning Ability and Off tracking - Motor Vehicles. Surface Vehicle Recommended Practice J695_201106, SAE International, Warrendale, PA.

Sayers, M.W. 1991. Exact Equations for Tractrix Curves Associated with Vehicle Off-tracking. Vehicle System Dynamics: International Journal of Vehicle Mechanics and Mobility, Taylor&Francis Group, **20**(3): 297 - 308.

Sun, Q., Xia, J., Foster, J., Falkmar, T., and Lee, H. 2017. Pursuing Precise Vehicle Movement Trajectory in Urban Residential Area Using Multi-GNSS RTK Tracking. Transportation Research Procedia, Elsevier, 25(2017): 2356-2372. doi:10.1016/j.trpro.2017.05.255 Avialable from https://www.sciencedirect.com/science/article/pii/S2352146517305628 [accessed 28 January 2018].

VSS (Association of Swiss Road and Traffic Engineers). 2003. Swiss Standard SN 640 105b: Verbreiterung der Fahrbahn in Kurven. Zürich, Swiss.

Wang, Y., and Linnett, J.A. 1995.Vehicle Kinematics and Its Application to Highway Design. ASCE Journal of Transportation Engineering, **121**(1): 63-74.

WHI (Western Highway Institute) 1970. Off-tracking Characteristics of Trucks and Truck Combinations. Research Committee Report. 3, San Bruno, California.

Woodrooffe, J.H.F., Morisset, L.E., and Smith, C.A.M. 1983. A Generalized Mathematical Solution for Transient Off Tracking of Single Vehicles and Truck Combinations. Division of Mechanical Engineering, Report No. 22878, National Research Council of Canada, Ottawa, Ontario.

**Table 1.** Error in X, Y terms with no pavement characteristics taken into account.

| Vehicle type | $H_{GPS}$ [m][a] | Average grade of pavement surface at test polygon [%][b] | Error in plan projection for X, Y [mm] |
|---|---|---|---|
| Volvo FH 500 (tractor) | 3.82 | 1.67 | 63.79 |
| Schmitz (semitrailer) | 4.13 | 1.73 | 71.45 |
| Renault T430 (3-axle truck) | 4.30 | 1.71 | 73.53 |
| Krone ZZ (central axle trailer) | 4.18 | 1.71 | 71.48 |
| Solaris URBINO (articulated bus) | 3.05 | 1.68 | 51.24 |
| IKARBUS IK 112 (single-unit bus) | 2.96 | 1.70 | 50.32 |

[a]$H_{GPS}$ represents the elevation difference between the center point of the GPS receiver mounted on the test vehicle and the pavement surface.
[b]Average grade of pavement surface is calculated based on the gradient vectors of 3D triangles covered by swept path envelopes. Since the steering paths are the same for all test vehicles, their swept path envelopes cover almost the same groups of 3D triangles representing the pavement surface.

## List of Figure Captions

Fig. 1. Test polygon layout: (a) steering path plan and (b) grading plan of the pavement surface.

Fig. 2. Dimensions of test vehicles and positions of installed GPS receivers.

Fig. 3. 3D view of electronic devices installed on the vehicle (Volvo tractor).

Fig. 4. Volvo FH 500 performing a 120° turning maneuver: (a) tablet computer, (b) high-resolution action camera, (c) laser designator mounted on Volvo front bumper, and (d) green laser beam.

Fig. 5. Installing GPS receivers atop the streamlined Volvo FH 500 tractor cabin.

Fig. 6. Imported and connected pairs of GPS coordinates by using the GPSLINE procedure in AutoCAD (for Volvo FH 500 tractor).

Fig. 7. Shifting of GPSLINES up the pavement triangles' gradient vectors.

Fig. 8. Adjusting MIDLINES' parameters (angle $\gamma$ and length d) to accurately trace the steering path with green laser beam (tractor base point).

Fig. 9. Retrieving the angle $\alpha$ between the MIDLINE and the tractor's longitudinal axis at the end of the entrance tangent (AVGLIN procedure).

Fig. 10. Analytically retrieving the angle $\alpha$ between the MIDLINE and the tractor's longitudinal axis (ALPHA procedure).

Fig. 11. Retrieving trailer trajectories from GPS coordinates.

Fig. 12. Overlapping vehicle blocks over GPSLINES (VEH2LINE procedure): a) overlapping Volvo FH 500 tractor blocks, b) overlapping SCHMITZ semitrailer blocks.

Fig. 13. Overview of the presented methodology and applied AutoLISP routines.

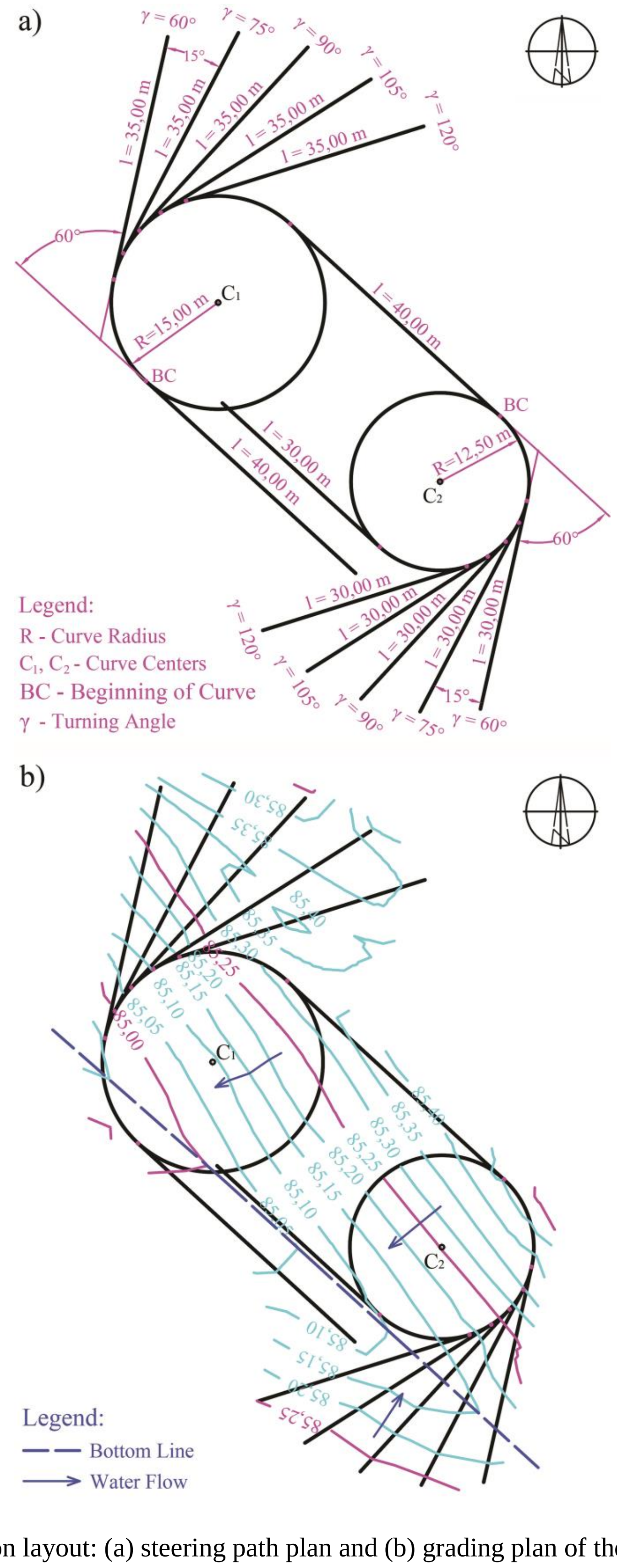


Fig. 1. Test polygon layout: (a) steering path plan and (b) grading plan of the pavement surface.

86x216mm (600 x 600 DPI)

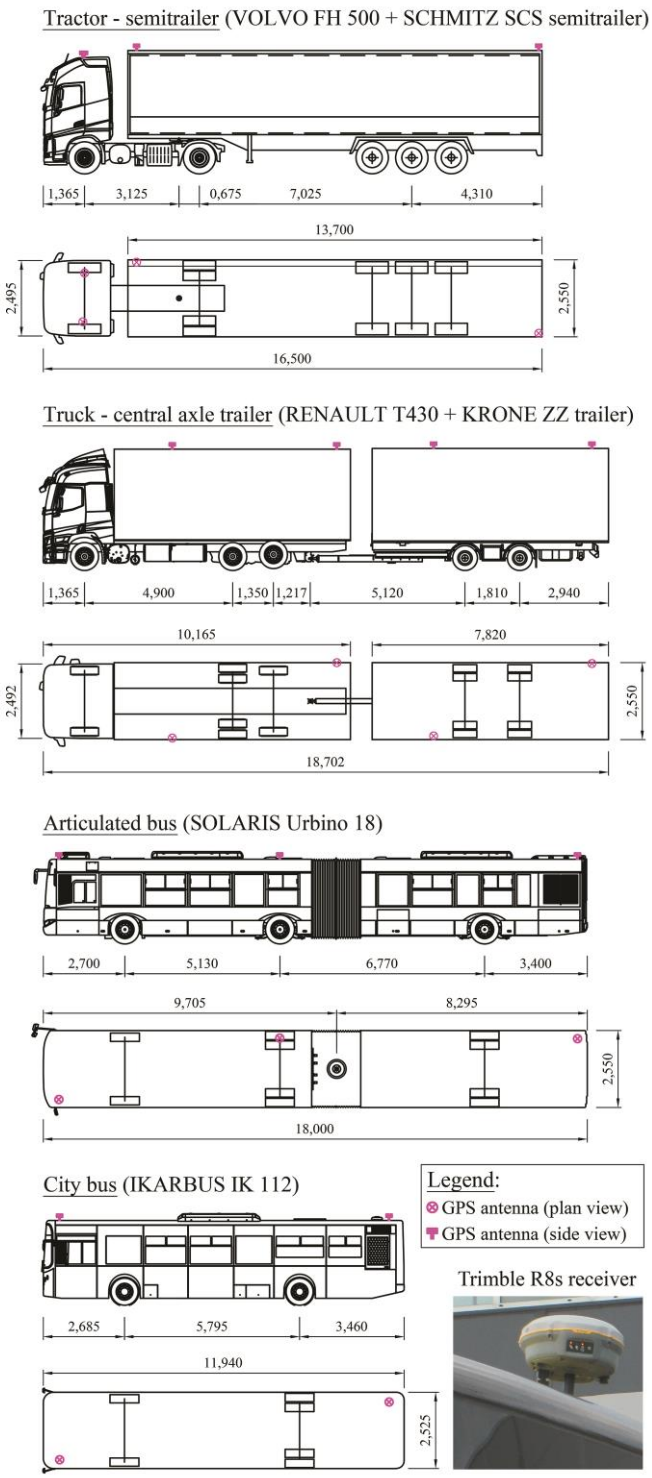


Fig. 2. Dimensions of test vehicles and positions of installed GPS receivers.

86x196mm (600 x 600 DPI)

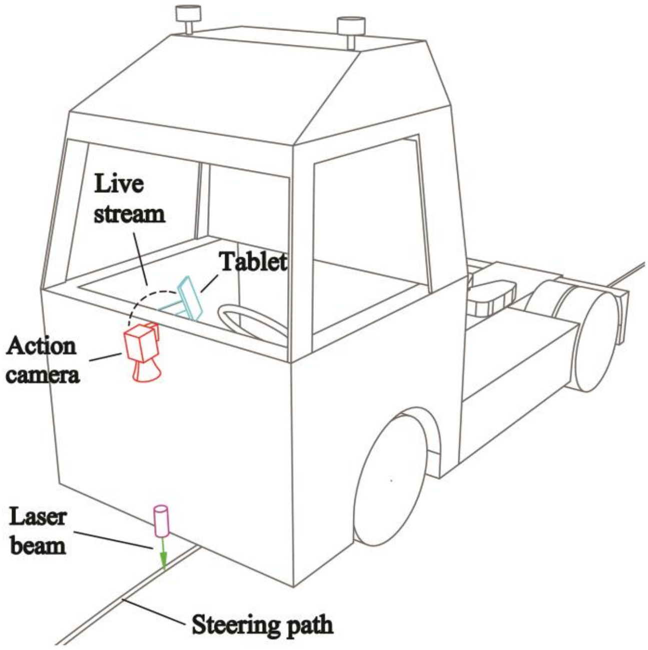


Fig. 3. 3D view of electronic devices installed on the vehicle (Volvo tractor).

86x86mm (600 x 600 DPI)


Fig. 4. Volvo FH 500 performing a 120° turning maneuver: (a) tablet computer, (b) high-resolution action camera, (c) laser designator mounted on Volvo front bumper, and (d) green laser beam.

182x110mm (600 x 600 DPI)

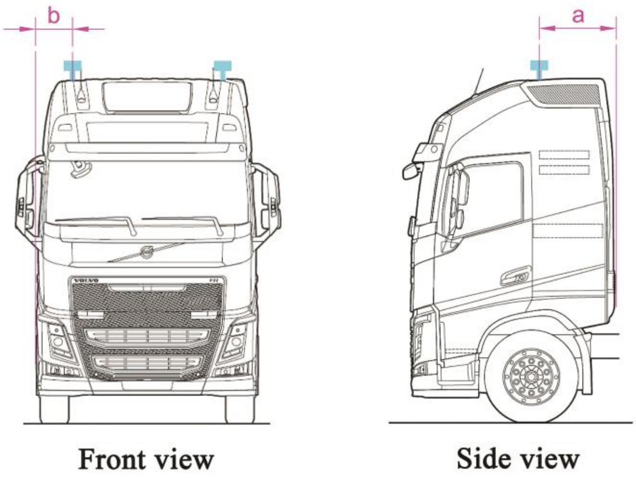


Fig. 5. Installing GPS receivers atop the streamlined Volvo FH 500 tractor cabin.

86x65mm (600 x 600 DPI)

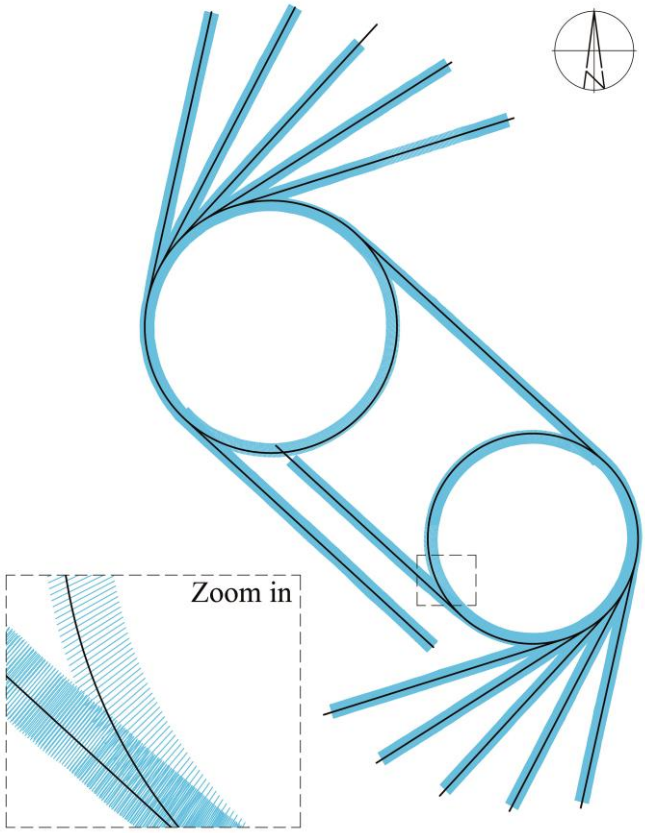


Fig. 6. Imported and connected pairs of GPS coordinates by using the GPSLINE procedure in AutoCAD (for Volvo FH 500 tractor).

86x111mm (600 x 600 DPI)

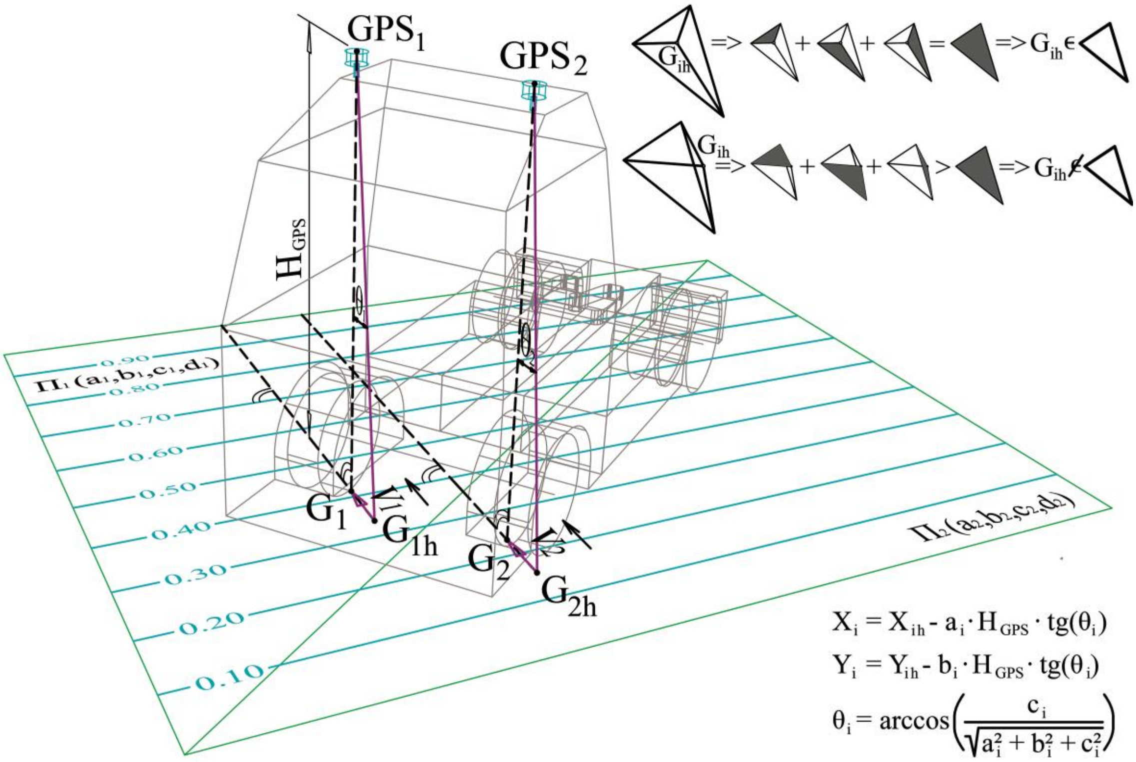


Fig. 7. Shifting of GPSLINES up the pavement triangles' gradient vectors.

182x123mm (600 x 600 DPI)

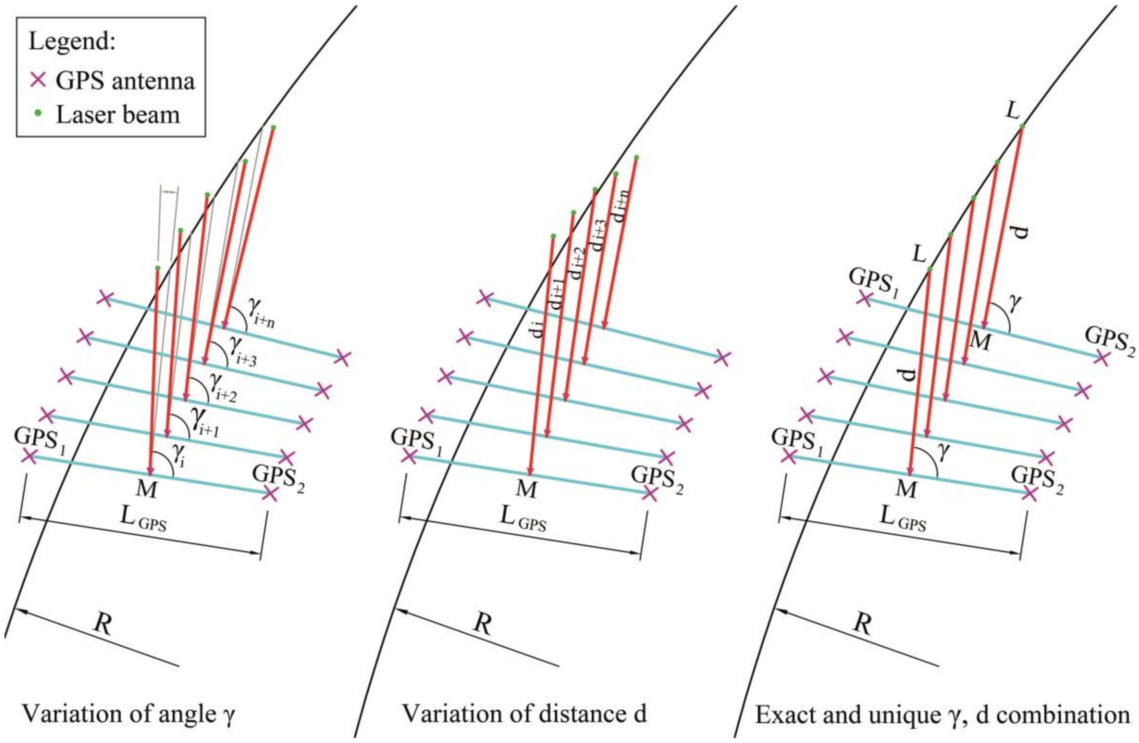


Fig. 8. Adjusting MIDLINES' parameters (angle γ and length d) to accurately trace the steering path with green laser beam (tractor base point).

182x118mm (600 x 600 DPI)

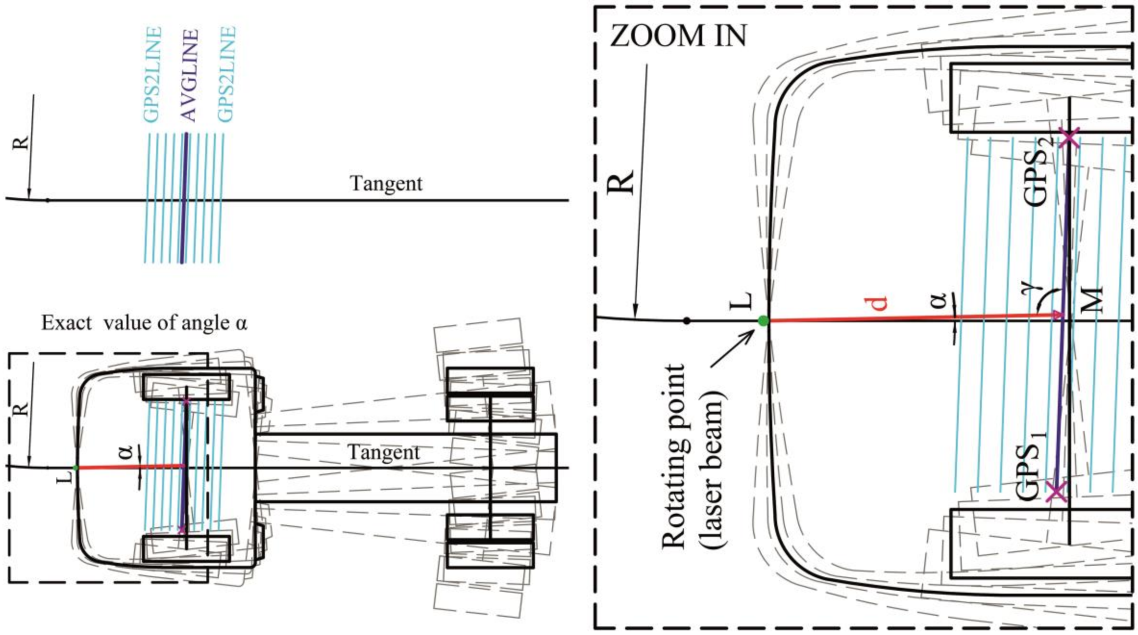


Fig. 9. Retrieving the angle $\alpha$ between the MIDLINE and the tractor's longitudinal axis at the end of the entrance tangent (AVGLIN procedure).

182x102mm (600 x 600 DPI)

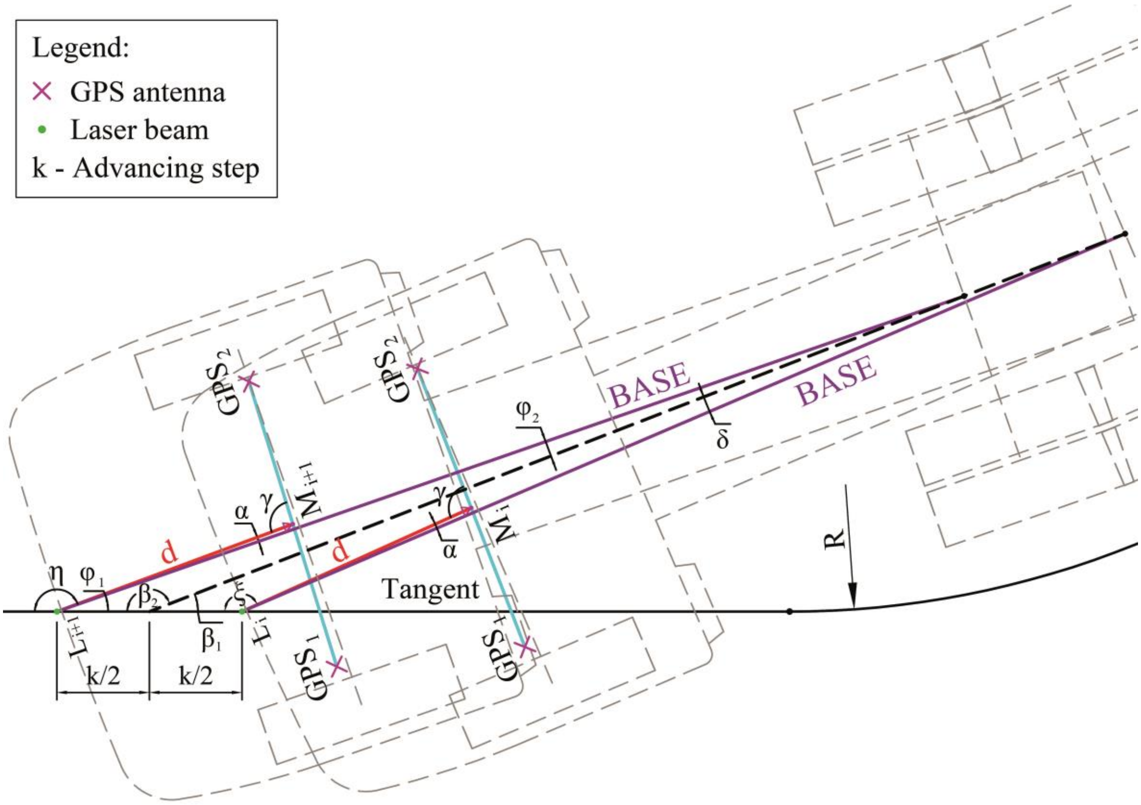


Fig. 10. Analytically retrieving the angle α between the MIDLINE and the tractor's longitudinal axis (ALPHA procedure).

182x129mm (600 x 600 DPI)

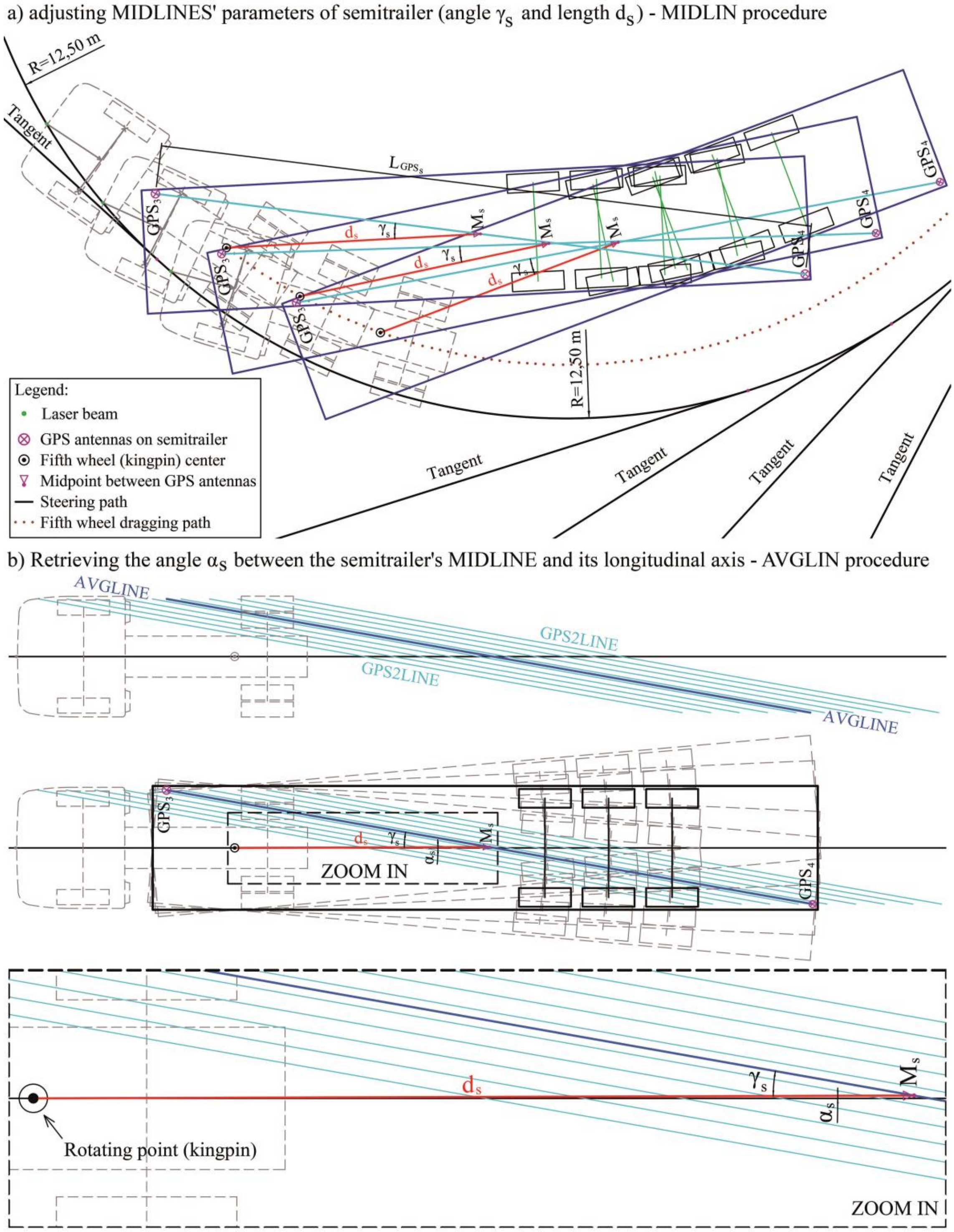


Fig. 11. Retrieving trailer trajectories from GPS coordinates.

182x237mm (600 x 600 DPI)

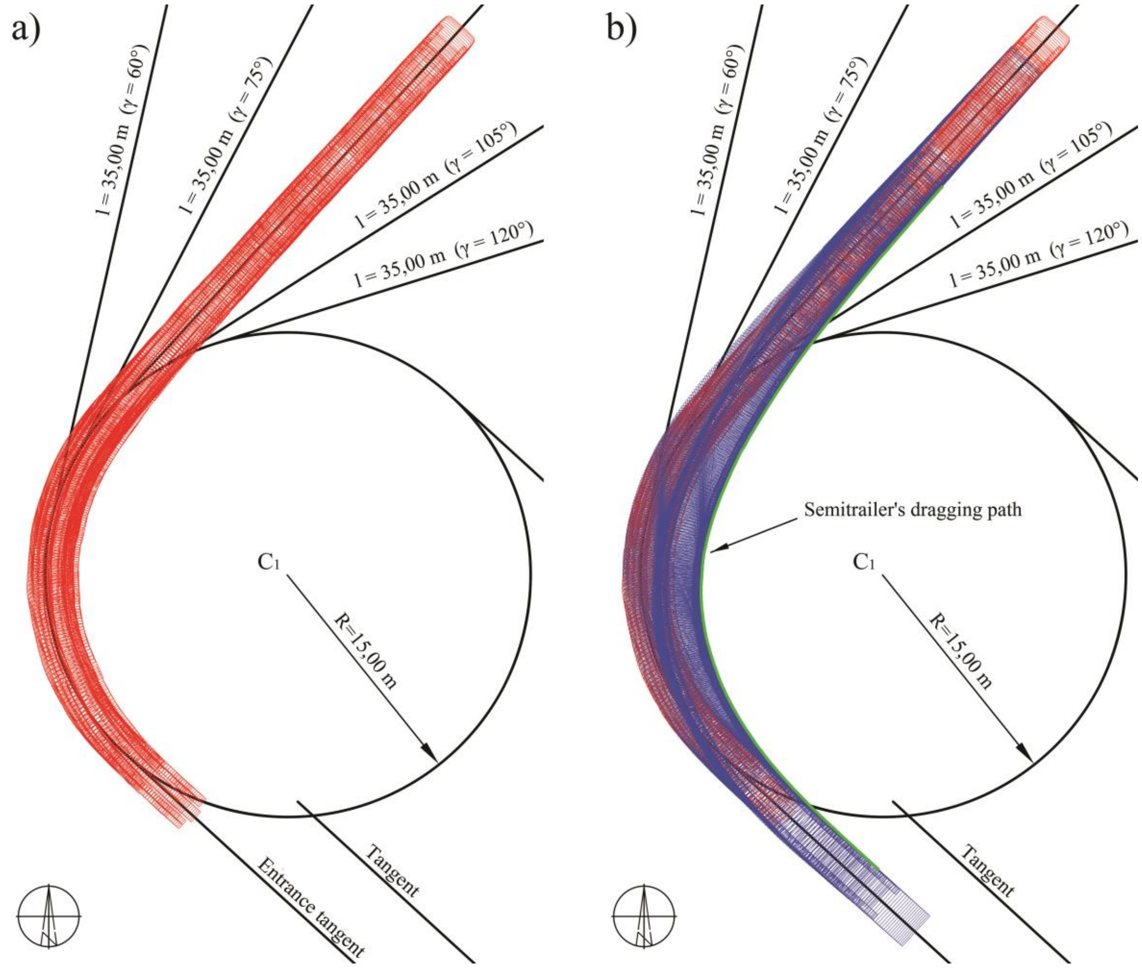


Fig. 12. Overlapping vehicle blocks over GPSLINES (VEH2LINE procedure): a) overlapping Volvo FH 500 tractor blocks, b) overlapping SCHMITZ semitrailer blocks.

182x154mm (600 x 600 DPI)

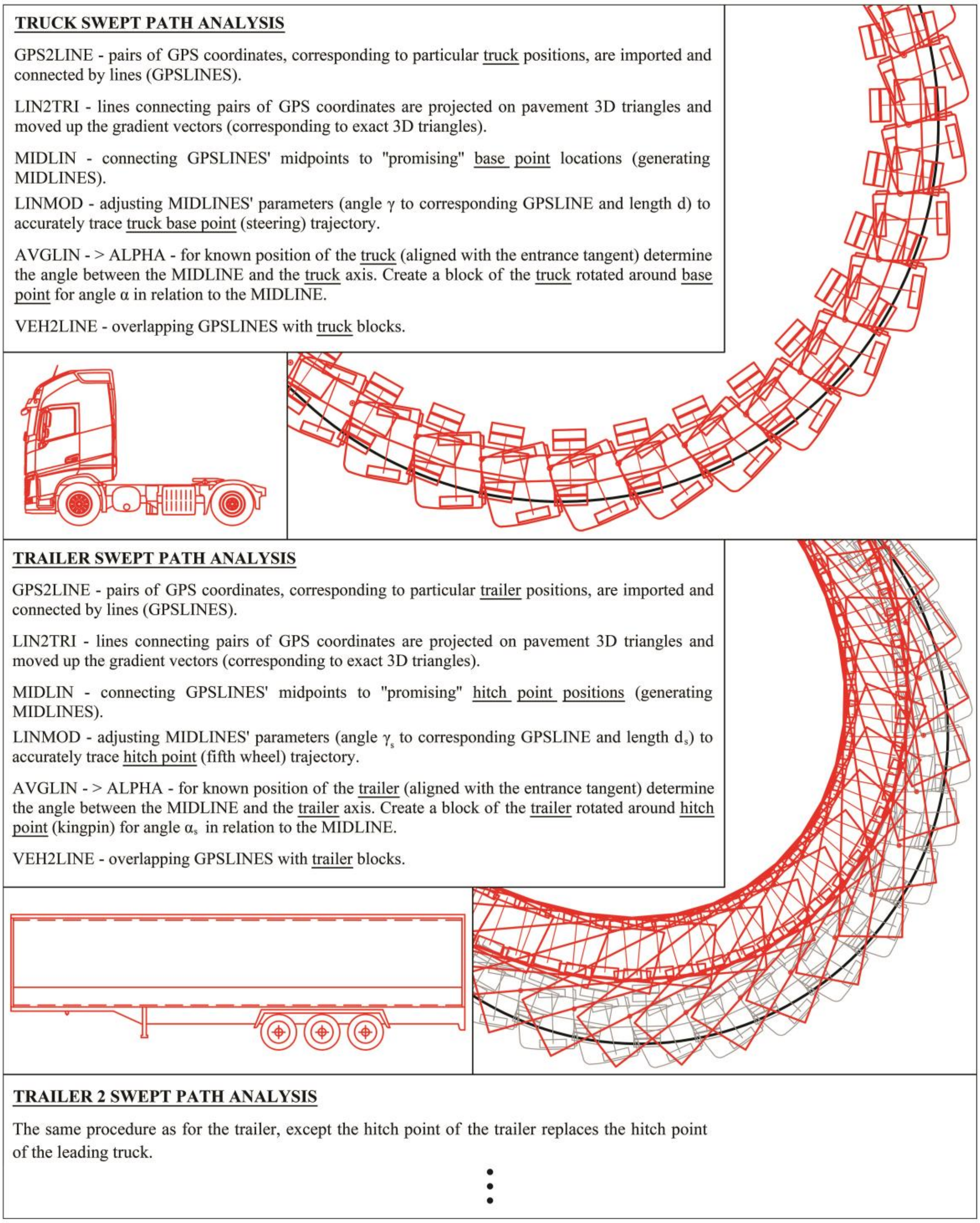


Fig. 13. Overview of the presented methodology and applied AutoLISP routines.

182x226mm (600 x 600 DPI)